RSC Advances

RSC Publishing

PAPER

View Article Online
View Journal | View Issue

One-pot green synthesis of nitrogen-doped carbon nanoparticles as fluorescent probes for mercury ions†

Cite this: *RSC Adv.*, 2013, **3**, 21691

Hong Huang,[a] Jing-Jing Lv,[a] Dan-Ling Zhou,[a] Ning Bao,[b] Yue Xu,[a] Ai-Jun Wang*[a] and Jiu-Ju Feng*[a]

Received 7th July 2013
Accepted 9th September 2013

DOI: 10.1039/c3ra43452d

www.rsc.org/advances

Herein, a simple, green, and low-cost way was developed in the synthesis of fluorescent nitrogen-doped carbon nanoparticles (FNCPs) with nitrogen content of 6.88%, using one-pot hydrothermal treatment of strawberry juice. The as-prepared FNCPs exhibited a maximum emission at 427 nm with a quantum yield of 6.3%, which could be specifically quenched by Hg^{2+}. This phenomenon was used to develop a fluorescent method for facile detection of Hg^{2+} with a linear range from 10 nM to 50 μM and a detection limit of 3 nM ($S/N = 3$), and further extended to measure environmental water samples with satisfactory recovery. This study provides a green strategy in the synthesis of FNCPs to detect Hg^{2+} with good performance.

Introduction

As a new kind of nanomaterial in the nanocarbon family, fluorescent carbon nanoparticles have drawn tremendous attention from recent research because of their unique optical/chemical properties. Unlike traditional organic dyes and semiconductor quantum dots, fluorescent carbon nanoparticles show distinguished properties such as stable photoluminescence, good biocompatibility and low toxicity.[1–3] It is believed that carbon nanoparticles are promising for a wide variety of applications, including bio-imaging,[4,5] optoelectronic devices,[6] sensors,[7–11] drug/gene delivery,[12,13] and photocatalysis.[14–17]

To date, many methods have been developed in the synthesis of carbon nanoparticles, including arc discharge,[18] laser ablation,[19] electrochemical,[20] chemical oxidation,[21,22] thermolysis,[23,24] ultrasonic,[25] and microwave methods.[26,27] Among them, hydrothermal synthesis strategy is considered to be a simple, direct, and efficient way to obtain carbon nanoparticles.[28]

Currently, more increasing efforts have been particularly focused on the preparation of fluorescent nitrogen-contained carbon nanoparticles (FNCPs) because of their broad applications in electrocatalysis, bioimaging, and sensors. For example, Zhu *et al.* synthesized bifunctional FNCPs by hydrothermal treatment of soy milk, which were used as electrocatalysts for oxygen reduction.[29] Wu and coworkers fabricated FNCPs from Bombyx mori silk for bioimaging.[30] Liu's group prepared FNCPs with grass as the carbon source, which were applied for the detection of Cu^{2+}.[31]

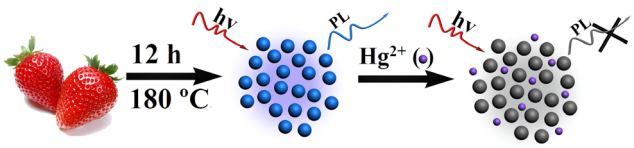

Scheme 1 Schematic illustration of the preparation process for the FNCPs and their application for Hg^{2+} detection.

Mercury ion (Hg^{2+}) is a widespread pollutant released through natural and human activities, which can accumulate in the human body through the food chain, leading to brain damage and other chronic diseases.[32] In recent years, various fluorescent probes have been prepared for the detection of Hg^{2+} based on biomaterials,[33] carbon nanoparticles,[34–36] metal nanoparticles,[37–39] and semiconductor quantum dots,[40,41] because fluorescence technique is a powerful tool with high sensitivity, high selectivity and real time monitoring. However, the tedious synthesis routes, high temperature, toxic agent, and high cost in the synthesis of these fluorescent probes limit their further applications. Thus, it is of great significance to develop novel fluorescent Hg^{2+} sensors for practical detection of Hg^{2+} in environmental samples.

Herein, a facile and green method was developed in the synthesis of water-soluble FNCPs by one-pot hydrothermal treating strawberry juice, which can be applied as an Hg^{2+} sensor (Scheme 1), even extending to the practical detection of Hg^{2+} in real water samples.

Experimental

Materials

Strawberries were bought from local supermarket and washed several times with water before use. NaCl, $CaCl_2$, $MnCl_2$, $MgCl_2$,

[a]*College of Geography and Environmental Science, College of Chemistry and Life Science, Zhejiang Normal University, Jinhua 321004, China. E-mail: ajwang@zjnu.cn; jjfeng@zjnu.cn; Fax: +86 579 82282269; Tel: +86 579 82282269*

[b]*School of Public Health, Nantong University, Nantong 226019, China*

† Electronic supplementary information (ESI) available. See DOI: 10.1039/c3ra43452d

$CuCl_2$, $CoCl_2$, $AlCl_3$, $Pb(NO_3)_2$, $FeCl_3$, $FeCl_2$, $CrCl_3$, $BaCl_2$, $ZnCl_2$, $CdCl_2$, $AgNO_3$, $NiCl_2$, CH_3COONa, $NaNO_3$, and $NaClO_4$ were purchased from Aladdin Ltd. (Shanghai, China). $(CH_3COO)_2Hg$, $HgCl_2$, and $Hg(NO_3)_2$ were obtained from Sinopharm Chemical Reagent Co., Ltd. (Shanghai, China). $Hg(ClO_4)_2$ were purchased from Sigma Aldrich (USA). All chemicals were of analytical grade and used as received without further purification. The water used in the whole experiments was purified through a Millipore system.

Preparation of FNCPs

The preparation of FNCPs was typically described as follows. 35 mL of strawberry juice was transferred into a 50 mL Teflon-lined autoclave and heated at 180 °C for 12 h. The large particles were removed by filtration with a 0.22 μm filter membrane and then centrifugation at 15 000 rpm for 30 min. The as-prepared FNCPs were finally dried under vacuum for 72 h and re-dispersed in water with a concentration of 1 mg mL^{-1} for further characterization and use.

Instrument for characterization

UV-Vis absorption spectra were recorded by a Lambda 950 UV-Vis spectrophotometer (Perkin-Elmer, USA). Fluorescence emission spectra were recorded by a LS-45 fluorescence spectrophotometer (Perkin-Elmer, UK). The fluorescence lifetime was measured using an Edinburgh FLS 920 photocounting system. X-ray photoelectron spectroscopy (XPS) was measured on a thermoelectron instrument (Thermo Scientific ESCALAB 250) with Al Kα X-ray radiation as the source for excitation (1486.8 eV, 500 μm). Transmission electron microscopy (TEM) was performed on a JEM-2100F transmission electron microscope using an acceleration voltage of 200 kV. Fourier transform infrared spectroscopy (FTIR) spectra of the samples were recorded in the form of KBr pellets with a Nicolet 670 FTIR spectrometer. Zeta potentials were measured on a Malvern Zetasizer Nano ZS dynamic light scattering system. The X-ray diffraction (XRD) patterns were obtained on a Philips PW3040/60 automatic powder diffractometer using Cu Kα radiation.

Fluorescence detection of Hg^{2+}

In a typical assay, 5 μL of the purified FNCPs solution was put into 1 mL of a phosphate solution (25 mM, pH 7.4), followed by the addition of different concentrations of Hg^{2+}. The solutions were mixed thoroughly and left to react for 10 min at room temperature, and then recorded the associated fluorescence quenching spectra.

Results and discussion

Characterization

The water-soluble FNCPs can be simply prepared by facile one-step hydrothermal treatment of strawberry juice. The solution of the FNCPs is clear yellow and displays a bright blue fluorescence under 365 nm UV light (insets 1–2 in Fig. 1A), which is different from the carbon particles obtained from orange juice.[42] As shown in Fig. 1A, the absorption of the FNCPs has an

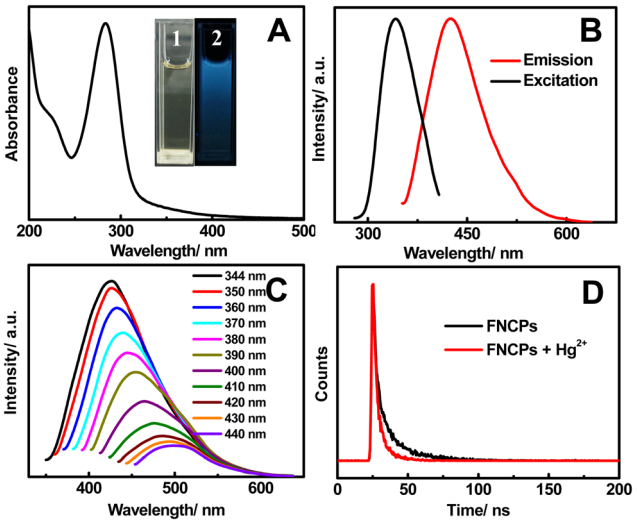

Fig. 1 (A) UV-Vis absorption spectrum of the as-prepared FNCPs. Inset shows the photographs of the FNCPs in aqueous solutions under visible light (1) and UV light (2). (B) Fluorescence excitation (black line) and emission (red line) spectra of the FNCPs. (C) Emission spectra of the FNCPs at different excitation wavelength from 350 to 440 nm. (D) Fluorescence decay traces of the FNCPs in the absence (black line) and presence (red line) of 50 μM Hg^{2+} upon excitation at 344 nm. The luminescence decay was fitted to a single-exponential decay.

obvious peak located at 283 nm, which represents the absorption of aromatic π orbitals.[25] Besides, the maximum emission peak is observed at 427 nm with a full width at half maximum of 95 nm in the emission spectra (Fig. 1B), when the excitation wavelength is 344 nm, suggesting narrow particle size distribution of the as-prepared FNCPs. Moreover, varying the excitation wavelength from 350 to 440 nm causes the emission peak gradually red shifted, as well as the decrease of the peak intensity (Fig. 1C). The excitation-dependent emission is an intrinsic property of the carbon particles.[43] The quantum yield of the FNCPs is 6.3%, using quinine sulfate (54% in 0.1 M H_2SO_4) as standard, which is comparable with the carbon particles reported previously.[44,45] The corresponding fluorescence lifetime is measured to be 7.6 ns, with excitation and emission wavelengths of 344 and 427 nm, respectively (Fig. 1D). This value is higher than those of the carbon particles reported in the literature.[12,46]

Typical TEM image shows that the as-prepared FNCPs are spherical in morphology, with an average diameter of 5.2 nm (Fig. 2A). Furthermore, the high-resolution TEM (HRTEM) image (Fig. 2B) shows the lattice plane with an interfringe distance of 0.254 nm, corresponding to the (100) planes of graphitic carbon.[47] Besides, the FNCPs have a diffraction peak centred at 22.6° in the typical XRD spectrum (Fig. 2C), indicating that the interlayer spacing of (002) diffraction peak is 0.39 nm. This value is larger than that of graphite (0.34 nm), possibly owing to the existence of oxygen-containing functional groups.[48]

The structures and components of the FNCPs are identified by FTIR and XPS experiments. As illustrated in Fig. 2D, the FTIR spectrum exhibits characteristic absorption bands of O–H and N–H stretching vibrations at 3400 cm^{-1}, C–H stretching

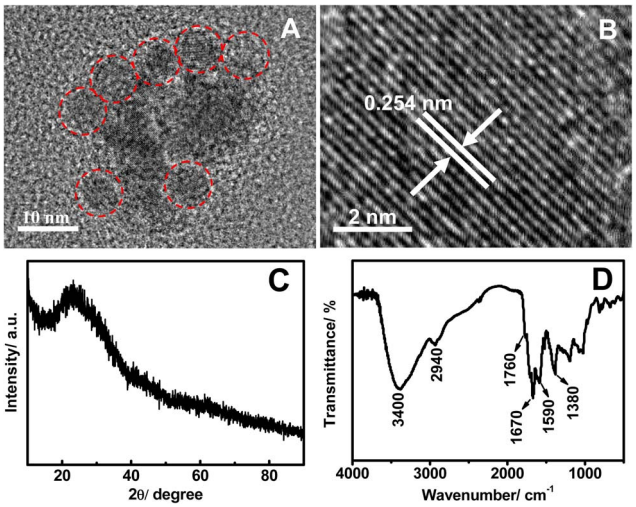

Fig. 2 Typical TEM image (A), HRTEM image (B), XRD pattern (C), and FTIR spectra (D) of the FNCPs.

vibrations at 2940 cm^{-1}, C=O stretching vibrations at 1760 and 1670 cm^{-1}, and C=C stretching vibrations at 1590 cm^{-1}.[30,49] Moreover, the bands in the range of 1030–1380 cm^{-1} suggest the presence of a large amount of C–O groups.[46] The zeta potential of the FNCPs was measured with a value of −18.3 mV, which further confirms the presence of hydroxyl and carboxylic groups on the surface of the FNCPs.

The XPS spectrum shows three strong peaks at 532.0, 401.1, and 286.1 eV, which are attributed to O_{1s}, N_{1s}, and C_{1s}, respectively (Fig. 3A). These results indicate that the FNCPs mainly contain C (67.46%), O (23.87%), and N (6.88%). The amount of N (6.88%) is higher than the carbon particles reported by Liu *et al.* and can be used for the surface passivation of carbon particles.[31] Specifically, the deconvolution of the C_{1s} spectrum (Fig. 3B) displays four peaks at 288.2, 286.3, 285.6, and 284.6 eV, which are assigned to the C=O, C–N, C–O, and C=C groups, respectively.[29] The O_{1s} spectrum (Fig. 3C) has two peaks at 533.0 and 531.7 eV, which are attributed to the C–OH/C–O–C and C–O groups, respectively.[45] The three peaks at 401.5, 400.5, and 399.5 eV in N_{1s} spectrum (Fig. 3D) are come from the N–H, N–$(C)_3$, and C–N–C groups, respectively.[50]

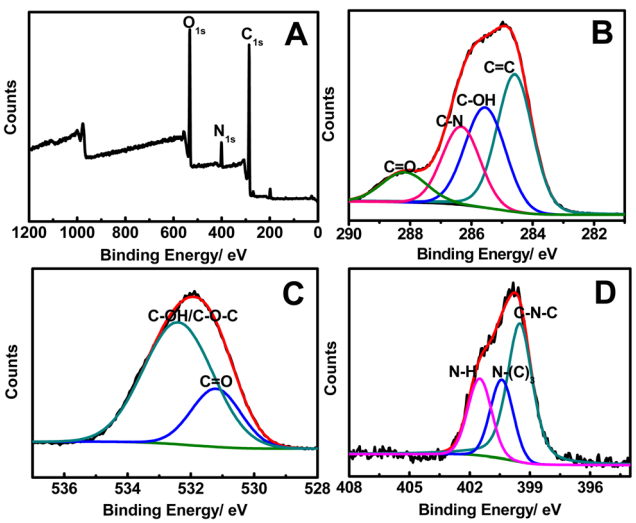

Fig. 3 The XPS (A), C_{1s} (B), O_{1s} (C), and N_{1s} (D) spectra of the as-obtained FNCPs.

As shown in Fig. 4A, the fluorescence intensity of the FNCPs remains almost constant in the presence of different concentrations of NaCl (up to 1 M), indicating high stability of the FNCPs even under high ionic strength environment. Meanwhile, varying the pH from 4 to 9 show no effects on the fluorescence intensities of the FNCPs (Fig. 4B), indicating the FNCPs are insensitive to the pH over the entire physiologically range, unlike the carbon particles reported by Shen's[51] and Shi's[52] groups. Furthermore, after irradiation for 7 h by using a 500 W Xe lamp, only a slight change in the fluorescence intensity is observed (Fig. 4C). Similar observation is obtained when the sample is stored for 3 months (Fig. 4D). These results indicate excellent photostability of the FNCPs, probably due to the electrostatic repulsions between the negatively charged nanoparticles. All these properties make the FNCPs particularly valuable for real applications in bio-labelling and bio-imaging.

Fluorescence detection of Hg^{2+}

Interestingly, we found that Hg^{2+} can obviously quench the fluorescence of the FNCPs, revealing that the FNCPs can be potentially used as an Hg^{2+} sensor. In the presence of 50 μM Hg^{2+}, time-dependent fluorescence spectra were recorded every 2 min within 12 min (Fig. 5). The fluorescence intensity at 427 nm decreases within 10 min and then remains constant with time, suggesting complete reaction between the FNCPs and Hg^{2+}. Thus, 10 min is chosen as the optimal reaction time.

The selectivity of the FNCPs to Hg^{2+} is also examined (Fig. 6), with other 15 metal ions (Ca^{2+}, Ag^{+}, Ni^{2+}, Cr^{3+}, Al^{3+}, Cu^{2+}, Ba^{2+}, Fe^{3+}, Pb^{2+}, Zn^{2+}, Fe^{2+}, Co^{2+}, Mg^{2+}, Mn^{2+}, or Cd^{2+}) tested as control. Hg^{2+} has the ability to quench the fluorescence

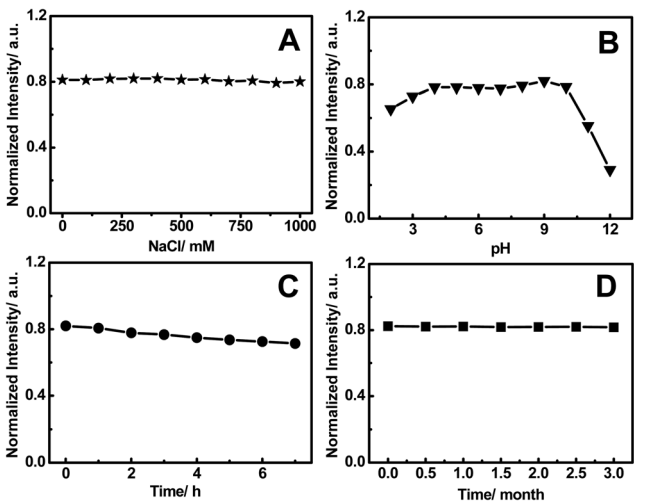

Fig. 4 (A) The relative fluorescence intensity at 427 nm (excitation at 344 nm) of the FNCPs in the NaCl solution. (B) Dependence of the fluorescence intensity on the pH values from 2 to 12. (C) The variation of the fluorescence intensity of the FNCPs under irradiation by a 500 W Xe lamp for different time intervals. (D) Photostability of the FNCPs as a function of the storage time.

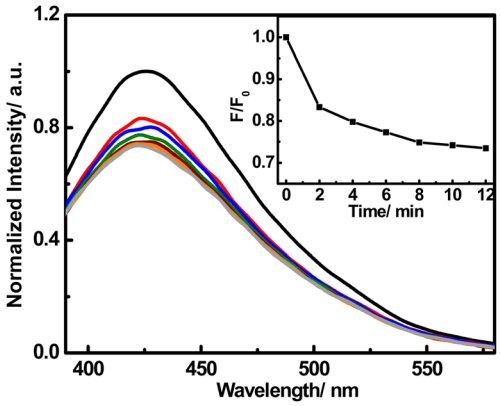

Fig. 5 Time-dependent fluorescence responses of the FNCPs to 50 μM Hg^{2+}. Inset shows the F/F_0 plotted against time in the presence of 50 μM Hg^{2+}, where F and F_0 are the fluorescence intensity of the FNCPs at 427 nm with and without Hg^{2+}, respectively.

intensity obviously, while the other metal ions have little or no quenching effects. Competitive experiments were also carried out to study the influence of other metal ions (Fig. S1†). The quenching caused by the mixture of Hg^{2+} (50 μM) with the other metal ions (100 μM) was similar to that caused solely by Hg^{2+} except very little interference of Cu^{2+}. These observations indicate high selectivity of the present fluorescent probe toward the detection of Hg^{2+}, owing to stronger affinity of Hg^{2+} than other metal ions toward the carboxylic, hydroxyl and amino groups on the surface of the FNCPs.[53] Furthermore, thus-formed FNCP–Hg^{2+} complexes would facilitate charge transfer and restrain the radiative recombination of excitons, leading to distinguished fluorescence quenching effects.[20]

In order to understand the interactions between the FNCPs and Hg^{2+}, UV-Vis absorption titration measurements were performed (Fig. S2†). Upon the successive addition of Hg^{2+}, an increase in absorption at 225 nm is observed, indicating the formation of the FNCP–Hg^{2+} complex.[35] The phenomenon is different from that reported by Pal and his coworkers,[35] because different functional groups are present on the carbon nanoparticles' surfaces.

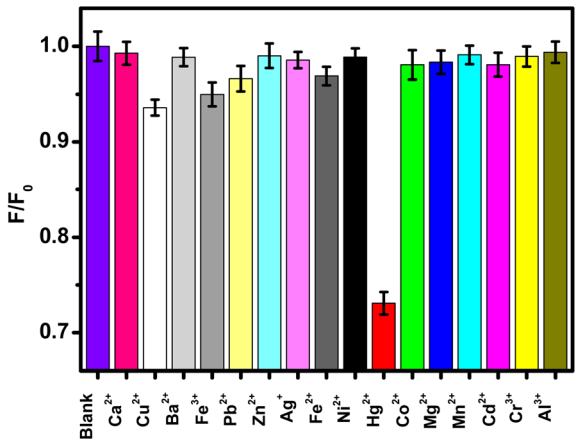

Fig. 6 Relative fluorescence intensity (F/F_0) of the FNCPs in phosphate solutions (25 mM, pH 7.4) with 50 μM different metal ions. F and F_0 correspond to the fluorescence intensity of the FNCPs with and without 50 μM of different metal ions.

Fluorescence lifetime measurements were conducted to gain further insight into the mechanism of fluorescence quenching of the FNCPs by Hg^{2+}. As shown in Fig. 1D, the fluorescence lifetime of the blank FNCPs is relatively high with a value of 7.6 ns, while the lifetime decays to 4.8 ns after the addition of Hg^{2+}. It indicates that the quenching is dynamic, further confirming an ultrafast electron transfer process in the FNCP–Hg^{2+} system.

Fig. S3† shows the fluorescence response of the FNCPs to 50 μM Hg^{2+} at various pH values. Evidently, the quenching efficiency is low under acidic media, where the surface binding carboxylic and amino groups are protonated, leading to the dissociation of the FNCP–Hg^{2+} complex. With the increase of pH, deprotonation of the carboxylic and amino groups occurs, which may strengthen the covalent bond between the FNCPs and Hg^{2+}, resulting in the significant decrease of the fluorescence intensity of the FNCPs. However, further increasing the pH value also causes a low quenching efficiency, because Hg^{2+} may be complexed by OH^- instead of the FNCPs under typical conditions. Furthermore, as mentioned above, varying pH values from 4 to 9 shows no effects on the fluorescence intensity of the system (Fig. 4B). All the results indicate that the carboxylic and amino groups on the surface of the FNCPs play a critical role for the sensitive and selective detection of Hg^{2+}.

The effects of different Hg^{2+} salts (chloride, nitrate, perchlorate and acetate salt of Hg^{2+}) on the emission of the FNCPs were also investigated. As displayed in Fig. S4,† all the Hg^{2+} salts display similar quenching effects. As control experiments, none of the Na^+ salts used show quenching of the fluorescence, demonstrating that Hg^{2+} is solely responsible for the quenching.

To evaluate the sensitivity of this system, different concentrations of Hg^{2+} within 50 μM were studied. As shown in Fig. 7, the fluorescence intensity of the FNCPs is sensitive to Hg^{2+} and decreases with the increase of Hg^{2+}. The quenching efficiency is fitted to the Stern–Volmer equation, $F_0/F = 1 + K_{SV}[Q]$, where K_{SV} is the Stern–Volmer quenching constant, [Q] is the concentration of analyte (Hg^{2+}), and F_0 and F are the fluorescence intensities at 427 nm in the absence and presence of Hg^{2+}, respectively. Fig. 7B shows two good linear ranges of 10–100 nM ($R = 0.9982$) and 1–50 μM ($R = 0.9851$), respectively. The limit of detection (LOD) is estimated to be 3 nM (at a signal-to-noise ratio of 3), which readily meets the Hg^{2+} detection requirement for drinking water by the European Union (5 nM, 1 ppb).[54]

To evaluate the performance of the FNCPs, other fluorescent methods of the detection of Hg^{2+} were provided for comparison (Table S1†). Evidently, the developed assay is superior, with the advantages of low detection limit and wide linear range, compared with other assays.

To test its practicality, the developed method was extended to determine the concentration of Hg^{2+} in environmental water samples from the Chuyang Lake on our campus. All the samples were filtered through a 0.22 μm membrane, followed by centrifugation at 15 000 rpm for 15 min to remove any

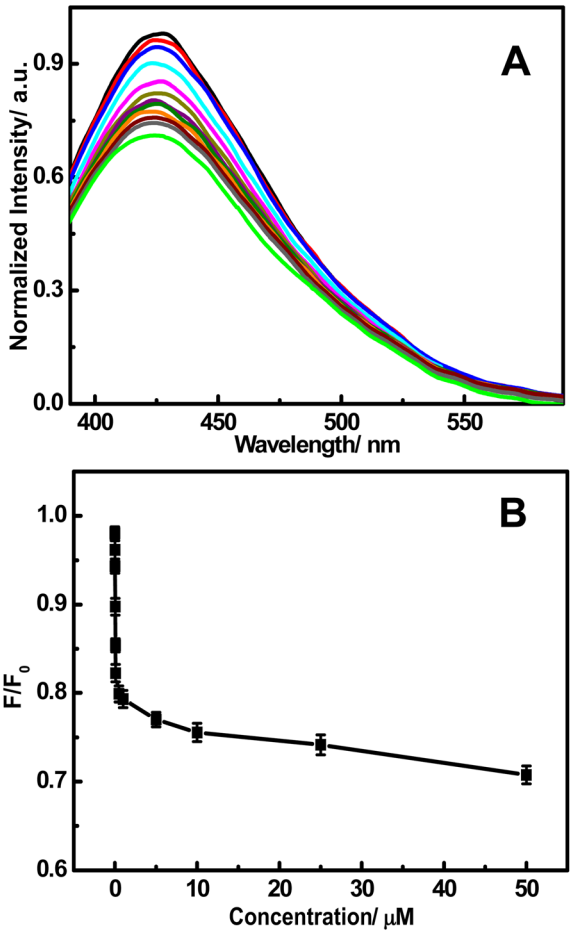

Fig. 7 (A) The fluorescence responses of the FNCPs in a phosphate solution (25 mM, pH 7.4) after the addition of different concentrations of Hg^{2+} (top to bottom): 0, 0.010, 0.025, 0.050, 0.075, 0.100, 0.500, 1.00, 5.00, 10.0, 25.0, and 50.0 μM. (B) Plot of the F/F_0 with the concentration of Hg^{2+}.

suspended particles. The fluorescence intensity of the FNCPs decreases when the samples have been spiked with standard solutions (Table S2†). The recoveries of Hg^{2+} in the spiked samples are in the range of 97–115%, illustrating little interference of the minerals, organics, and bacteria present in the samples. These results demonstrate that this sensing system has great potential for quantitative detection of Hg^{2+} in environmental samples.

Conclusion

In summary, a facile, simple, and low-cost method was developed for the green preparation of water-soluble FNCPs using strawberry juice as a carbon source. The as-prepared FNCPs was used for sensitive and selective detection of Hg^{2+} with wide linear range from 10 nM to 50 μM and low detection limit of 3 nM ($S/N = 3$), based on the quenching effects of Hg^{2+}. This approach was further extended to the practical assay of Hg^{2+} in water samples. For the easy production of stable and strong fluorescence of the FNCPs, we believe that the FNCPs would have many potential applications in chemistry and biology.

Acknowledgements

This work was financially supported by the NSFC (no. 20905021, 21075070, 21175118, 21275130, 21375066 and 21275131) and the Foundation of the Ministry of Education of China for Returned Scholars (A.J.W. and J.J.F.), and preferentially financing projects of scientific and technological activities of overseas students in Zhejiang province (no. (2011)-443, for J.J.F.), and National Students' innovation and entrepreneurship training program of Zhejiang Normal University (Y.X).

References

1 H. Li, Z. Kang, Y. Liu and S.-T. Lee, *J. Mater. Chem.*, 2012, **22**, 24230–24253.
2 S. N. Baker and G. A. Baker, *Angew. Chem., Int. Ed.*, 2010, **49**, 6726–6744.
3 P. G. Luo, S. Sahu, S.-T. Yang, S. K. Sonkar, J. Wang, H. Wang, G. E. LeCroy, L. Cao and Y.-P. Sun, *J. Mater. Chem. B*, 2013, **1**, 2116–2127.
4 S. C. Ray, A. Saha, N. R. Jana and R. Sarkar, *J. Phys. Chem. C*, 2009, **113**, 18546–18551.
5 L. Zhou, Z. Li, Z. Liu, J. Ren and X. Qu, *Langmuir*, 2013, **29**, 6396–6403.
6 X. Guo, C.-F. Wang, Z.-Y. Yu, L. Chen and S. Chen, *Chem. Commun.*, 2012, **48**, 2692–2694.
7 Y. Dong, R. Wang, G. Li, C. Chen, Y. Chi and G. Chen, *Anal. Chem.*, 2012, **84**, 6220–6224.
8 W. Shi, Q. Wang, Y. Long, Z. Cheng, S. Chen, H. Zheng and Y. Huang, *Chem. Commun.*, 2011, **47**, 6695–6697.
9 Y. Dong, G. Li, N. Zhou, R. Wang, Y. Chi and G. Chen, *Anal. Chem.*, 2012, **84**, 8378–8382.
10 W. T. Huang, Y. Shi, W. Y. Xie, H. Q. Luo and N. B. Li, *Chem. Commun.*, 2011, **47**, 7800–7802.
11 X. Ran, H. Sun, F. Pu, J. Ren and X. Qu, *Chem. Commun.*, 2013, **49**, 1079–1081.
12 C. Liu, P. Zhang, X. Zhai, F. Tian, W. Li, J. Yang, Y. Liu, H. Wang, W. Wang and W. Liu, *Biomaterials*, 2012, **33**, 3604–3613.
13 Q. Wang, X. Huang, Y. Long, X. Wang, H. Zhang, R. Zhu, L. Liang, P. Teng and H. Zheng, *Carbon*, 2013, **59**, 192–199.
14 H. Li, X. He, Z. Kang, H. Huang, Y. Liu, J. Liu, S. Lian, C. H. A. Tsang, X. Yang and S.-T. Lee, *Angew. Chem., Int. Ed.*, 2010, **49**, 4430–4434.
15 H. Li, R. Liu, Y. Liu, H. Huang, H. Yu, H. Ming, S. Lian, S.-T. Lee and Z. Kang, *J. Mater. Chem.*, 2012, **22**, 17470–17475.
16 L. Cao, S. Sahu, P. Anilkumar, C. E. Bunker, J. Xu, K. A. S. Fernando, P. Wang, E. A. Guliants, K. N. Tackett and Y.-P. Sun, *J. Am. Chem. Soc.*, 2011, **133**, 4754–4757.
17 H. Li, R. Liu, S. Lian, Y. Liu, H. Huang and Z. Kang, *Nanoscale*, 2013, **5**, 3289–3297.
18 X. Xu, R. Ray, Y. Gu, H. J. Ploehn, L. Gearheart, K. Raker and W. A. Scrivens, *J. Am. Chem. Soc.*, 2004, **126**, 12736–12737.
19 S.-L. Hu, K.-Y. Niu, J. Sun, J. Yang, N.-Q. Zhao and X.-W. Du, *J. Mater. Chem.*, 2009, **19**, 484–488.

20 Y.-L. Zhang, L. Wang, H.-C. Zhang, Y. Liu, H.-Y. Wang, Z.-H. Kang and S.-T. Lee, *RSC Adv.*, 2013, **3**, 3733–3738.
21 Y. Dong, N. Zhou, X. Lin, J. Lin, Y. Chi and G. Chen, *Chem. Mater.*, 2010, **22**, 5895–5899.
22 H. Tao, K. Yang, Z. Ma, J. Wan, Y. Zhang, Z. Kang and Z. Liu, *Small*, 2012, **8**, 281–290.
23 K. Qu, J. Wang, J. Ren and X. Qu, *Chem.–Eur. J.*, 2013, **19**, 7243–7249.
24 Y. Dong, H. Pang, H. B. Yang, C. Guo, J. Shao, Y. Chi, C. M. Li and T. Yu, *Angew. Chem., Int. Ed.*, 2013, **52**, 1–6.
25 H. Li, X. He, Y. Liu, H. Huang, S. Lian, S.-T. Lee and Z. Kang, *Carbon*, 2011, **49**, 605–609.
26 X. Wang, K. Qu, B. Xu, J. Ren and X. Qu, *J. Mater. Chem.*, 2011, **21**, 2445–2450.
27 Q. Wang, H. Zheng, Y. Long, L. Zhang, M. Gao and W. Bai, *Carbon*, 2011, **49**, 3134–3140.
28 Q. Liang, W. Ma, Y. Shi, Z. Li and X. Yang, *Carbon*, 2013, **60**, 421–428.
29 C. Zhu, J. Zhai and S. Dong, *Chem. Commun.*, 2012, **48**, 9367–9369.
30 Z. L. Wu, P. Zhang, M. X. Gao, C. F. Liu, W. Wang, F. Leng and C. Z. Huang, *J. Mater. Chem. B*, 2013, **1**, 2868–2873.
31 S. Liu, J. Tian, L. Wang, Y. Zhang, X. Qin, Y. Luo, A. M. Asiri, A. O. Al-Youbi and X. Sun, *Adv. Mater.*, 2012, **24**, 2037–2041.
32 T. W. Clarkson and L. Magos, *Crit. Rev. Toxicol.*, 2006, **36**, 609–662.
33 X. Yang, Y. Zhu, P. Liu, L. He, Q. Li, Q. Wang, K. Wang, J. Huang and J. Liu, *Anal. Methods*, 2012, **4**, 895–897.
34 Y. Guo, Z. Wang, H. Shao and X. Jiang, *Carbon*, 2013, **52**, 583–589.
35 H. Chakraborti, S. Sinha, S. Ghosh and S. K. Pal, *Mater. Lett.*, 2013, **97**, 78–80.
36 L. Zhou, Y. Lin, Z. Huang, J. Ren and X. Qu, *Chem. Commun.*, 2012, **48**, 1147–1149.
37 D. Hu, Z. Sheng, P. Gong, P. Zhang and L. Cai, *Analyst*, 2010, **135**, 1411–1416.
38 T. Zhou, Y. Huang, Z. Cai, F. Luo, C. J. Yang and X. Chen, *Nanoscale*, 2012, **4**, 5312–5315.
39 H. Wei, Z. Wang, L. Yang, S. Tian, C. Hou and Y. Lu, *Analyst*, 2010, **135**, 1406–1410.
40 A. N. Liang, L. Wang, H.-Q. Chen, B.-B. Qian, B. Ling and J. Fu, *Talanta*, 2010, **81**, 438–443.
41 J. Duan, L. Song and J. Zhan, *Nano Res.*, 2009, **2**, 61–68.
42 S. Sahu, B. Behera, T. K. Maiti and S. Mohapatra, *Chem. Commun.*, 2012, **48**, 8835–8837.
43 B. Chen, F. Li, S. Li, W. Weng, H. Guo, T. Guo, X. Zhang, Y. Chen, T. Huang, X. Hong, S. You, Y. Lin, K. Zeng and S. Chen, *Nanoscale*, 2013, **5**, 1967–1971.
44 Y. Yang, J. Cui, M. Zheng, C. Hu, S. Tan, Y. Xiao, Q. Yang and Y. Liu, *Chem. Commun.*, 2012, **48**, 380–382.
45 W. Lu, X. Qin, S. Liu, G. Chang, Y. Zhang, Y. Luo, A. M. Asiri, A. O. Al-Youbi and X. Sun, *Anal. Chem.*, 2012, **84**, 5351–5357.
46 X. Jia, J. Li and E. Wang, *Nanoscale*, 2012, **4**, 5572–5575.
47 W. Kwon and S.-W. Rhee, *Chem. Commun.*, 2012, **48**, 5256–5258.
48 J. Peng, W. Gao, B. K. Gupta, Z. Liu, R. Romero-Aburto, L. Ge, L. Song, L. B. Alemany, X. Zhan, G. Gao, S. A. Vithayathil, B. A. Kaipparettu, A. A. Marti, T. Hayashi, J.-J. Zhu and P. M. Ajayan, *Nano Lett.*, 2012, **12**, 844–849.
49 Y. Dong, R. Wang, H. Li, J. Shao, Y. Chi, X. Lin and G. Chen, *Carbon*, 2012, **50**, 2810–2815.
50 S. Liu, J. Tian, L. Wang, Y. Luo, J. Zhai and X. Sun, *J. Mater. Chem.*, 2011, **21**, 11726–11729.
51 L. Shen, L. Zhang, M. Chen, X. Chen and J. Wang, *Carbon*, 2013, **55**, 343–349.
52 W. Shi, X. Li and H. Ma, *Angew. Chem.*, 2012, **124**, 6538–6541.
53 X. Qin, W. Lu, A. M. Asiri, A. O. Al-Youbi and X. Sun, *Sens. Actuators, B*, 2013, **184**, 156–162.
54 L. Shang, L. Yang, F. Stockmar, R. Popescu, V. Trouillet, M. Bruns, D. Gerthsen and G. U. Nienhaus, *Nanoscale*, 2012, **4**, 4155–4160.

